# Quasi-helical Symmetry at Finite Aspect Ratio

C. Nührenberg[1], M.I. Mikhailov[2], J. Nührenberg[1], V.D. Shafranov[2]
[1]Max-Planck-Institut für Plasmaphysik, EURATOM Association
D-17491 Greifswald, Germany
[2]Russian Research Centre "Kurchatov Institute", Moscow, Russia

*Abstract.* Computational stellarator optimization is used to create a configuration which is quasi-helically symmetric at finite aspect ratio. For the aspect ratio per period chosen ($\approx 2$) this procedure results in benign properties throughout the plasma volume.

## Introduction

Previously, stellarator optimizations of quasi-symmetric configurations have been performed with respect to the complete plasma volume, see e.g. [1, 2]. Since it was on one hand proven that quasi-symmetries cannot be achieved exactly over the entire plasma volume and, on the other hand, that they can be strictly obtained on one flux surface [3], a different option for optimization is to choose a flux surface at finite aspect ratio and realize quasi-symmetry there. This option is investigated here: The boundary of the quasi-helically symmetric configuration obtained in [1] is selected and a 47-dimensional configurational space comprising boundary Fourier coefficients with poloidal mode numbers $m$ and toroidal mode numbers $|n|$ up to 3 is used to try to achieve quasi-helical symmetry at a toroidal aspect ratio $\approx 12$ corresponding to an aspect ratio per period of $\approx 2$. The result is the subject of this brief communication.

## Results

Figure 1 shows structures of the strength of $B = \sum_{mn} B_{mn} \cos 2\pi(m\theta + n\phi)$ [with $\theta$ and $\phi$ the poloidal and toroidal angle-like magnetic coordinates] in terms of its small Fourier components, $B_{mn}$ (the two largest components, $B_{0\,0}$ and $B_{1\,-1}$, are not shown). While in the configuration of [1] all coefficients tend to get larger with increasing flux this is clearly the case only for the helically symmetric coefficients in the configuration obtained here; the coefficients perturbing the quasi-symmetry form two classes: those corresponding to the optimization space chosen exhibit the quasi-symmetry at the plasma boundary rather perfectly; the amplitudes of higher-order Fourier components not corresponding to the optimization space remain at the few per mill level.

The comparison of the two configurations seen in Fig. 2 shows that the flux surface geometry resulting from the optimization performed here is well-behaved. In cylindrical coordinates $(R, \varphi, Z)$, the plasma boundary is defined by the two functions $R(u, v) = \sum_{mn} R_{mn} \cos 2\pi(mu - nv)$ and $Z(u, v) = \sum_{mn} Z_{mn} \cos 2\pi(mu - nv)$, where $v = N_p\varphi/(2\pi)$, $N_p = 6$, and $u$ a poloidal parametrization. The boundary coefficients, $R_{mn}$ and $Z_{mn}$, of the cases discussed here are given in Tables I and II. No constraints on the rotational transform and the magnetic well have been used; as a result, the rotational transform is slightly larger (see Fig. 3), the magnetic well slightly deeper than in the configuration of [1].

In the context of quasi-symmetry the characterization of neoclassical transport properties is of particular relevance. Fig. 4 shows that the equivalent neoclassical ripple (characterizing the level of the so-called $1/\nu$ transport, see, e.g., [4, 5] and, specifically, $\epsilon^{\frac{3}{2}}$ in [6]) is of similar smallness in both configurations. From Fig. 5, it is seen that the bootstrap current [7, 8] is similar, and from Fig. 6 that the collisionless loss of $\alpha$-particles is small, but a factor of about 2 smaller for particles started at half the plasma radius and a factor of about 4 smaller for particles started at 0.7 of the plasma radius in the configuration obtained here.

**Conclusion**

It appears that the procedure used here to obtain nearly quasi-symmetric configurations is viable, too. The computational optimization was performed with a NAG routine (E04UCF), i.e. exploiting the smoothness of the problem. A genetic algorithm [9] was used to verify the global nature of the optimum found.

**Acknowledgment**

This work was supported in part by the Russian Foundation for Basic Research, project no 09-02-0142-a and by grant 2457.2008.2 of President of Russian Federation for state support of leading scientific school.

## References


[1] J. Nührenberg and R. Zille, Physics Letters A **129** 1988, 113.

[2] J. Nührenberg et al, in Theory of Fusion Plasmas Editrice Compositori, Bologna 1994, 3.

[3] D.A. Garren and A.H. Boozer, Phys. Fluids B **3** 1991, 2805.

[4] A.A. Galeev and R.Z. Sagdeev, Zh. Eksp. Teor. Fiz. **53** 1967, 348 [Sov. Phys. – JETP **26** 1968, 233].

[5] W. Lotz and J. Nührenberg, Phys. Fluids **31** 1988, 2984.

[6] V.V. Nemov et al, Plasma Phys. Contr. Fusion **45** 2003, 43.

[7] R.J. Bickerton, J.W. Connor, and J.B. Taylor, Nat. Phys. Sci. **239** 1971, 110.

[8] W.A. Cooper et al, Plasma Phys. Contr. Fusion **44** 2002, B357.

[9] A. Ben Haj-Yedder, in Automatic Differentiation of Algorithms: From Simulation to Optimization, edited by G. Corliss, C. Faure, A. Griewank and L. Hascoet (Springer, Berlin, 2002).

## Figure captions

Fig. 1. Small Fourier coefficients of the magnetic field strength in magnetic coordinates of two quasi-helical configurations, top from [1] and bottom obtained here; $B_{0\,0} \approx 1.3$ and $B_{1\,-1} \approx -0.18$ at the boundary (top), $B_{0\,0} \approx 1.4$ and $B_{1\,-1} \approx -0.22$ at the boundary (bottom) are not shown; —— low-m coefficients perturbing the quasi-symmetry; $----$ quasi-symmetric coefficients; $\times\times\times$ high-m coefficients perturbing the quasi-symmetry. The 17 largest of the small coefficients are shown.

Top: —— : (3, -2), (2, -3), (2, 0), (0, -1), (1, 1), (3, 0), (1, -2), (2, -1); $----$: (3, -3), (4, -4), (2, -2); $\times\times\times$: (5, -4), (4, -2), (4, -1), (7, -6), (6, -5), (4, -3).

Bottom: —— : (0, -1), (1, -2), (1, 0), (2, -1), (2, -3), (1, -3), (3, -4); $----$: (3, -3), (4, -4), (5, -5), (6, -6), (7, -7), (8, -8), (2, -2); $\times\times\times$: (5, -4), (4, -5), (7, -8).

Fig. 2. Magnetic surfaces at the beginning, quarter of and half of a period for two quasi-helically symmetric configurations; top from [1], bottom obtained here. The boundary coefficients of the latter are given in Tables I and II.

Fig. 3 Rotational transform vs. flux label; solid line: configuration found here, dash-dotted line: [1].

Fig. 4. Equivalent neoclassical ripple $\epsilon$ (here used in the form $\epsilon^{\frac{3}{2}}$ vs. flux surface label; solid line: configuration found here, dash-dotted line: [1]. The spike in $\epsilon$ from [1] is due to the incidental resonance, $\iota_{\text{period}} = \frac{1}{4}$.

Fig. 5. Structural factor of the bootstrap current vs. flux surface label; solid line: configuration found here, dash-dotted line: [1]. The difference in the structural factor at large flux label is again due to $\iota_{\text{period}} = \frac{1}{4}$ near the boundary.

Fig. 6. Four different loss histories of 1000 collisionless $\alpha$-particles started (randomly distributed in the angular variables and pitch angle) at half and 0.7 of the plasma radius. Normalization: plasma volume $10^3$ m$^3$, magnetic field 5 T. Each symbol marks the loss of one particle in a cumulative way. The straight lines indicate the fractions of reflected particles (in each case the lower line corresponds to half the plasma radius); dash-dotted lines, $\Box$ and *: configuration found here; solid lines, $\circ$ and $\diamond$: [1].

**Tables**

| n | $m$ | | | |
|---|---|---|---|---|
| | 0 | 1 | 2 | 3 |
| -3 | 0 | 0.0026 | 0.0003 | $-0.0008$ |
| -2 | 0 | $-0.0027$ | $-0.01$ | 0.0011 |
| -1 | 0 | 0.0404 | $-0.006$ | $-0.0071$ |
| 0 | 11 | 1.1761 | 0.0463 | $-0.0317$ |
| 1 | 0.6833 | $-0.5672$ | 0.242 | 0.0315 |
| 2 | 0.0214 | $-0.0765$ | 0.0665 | $-0.0752$ |
| 3 | 0.0019 | 0.0058 | 0.0322 | $-0.0017$ |

**Table I.** *$R$ boundary coefficients of a 6-periodic case optimized for quasi-helical symmetry on the plasma boundary.*

| n | $m$ | | | |
|---|---|---|---|---|
| | 0 | 1 | 2 | 3 |
| -3 | 0 | 0.0001 | 0.0003 | $-0.0006$ |
| -2 | 0 | $-0.0025$ | $-0.0081$ | $-0.0003$ |
| -1 | 0 | 0.033 | $-0.0062$ | $-0.0049$ |
| 0 | 0 | 0.8239 | 0.0547 | $-0.0144$ |
| 1 | $-0.8546$ | 0.3713 | 0.2141 | $-0.0007$ |
| 2 | $-0.0242$ | 0.0791 | $-0.0244$ | $-0.0177$ |
| 3 | $-0.0074$ | 0.0012 | $-0.025$ | $-0.012$ |

**Table II.** *$Z$ boundary coefficients of a 6-periodic case optimized for quasi-helical symmetry on the plasma boundary.*

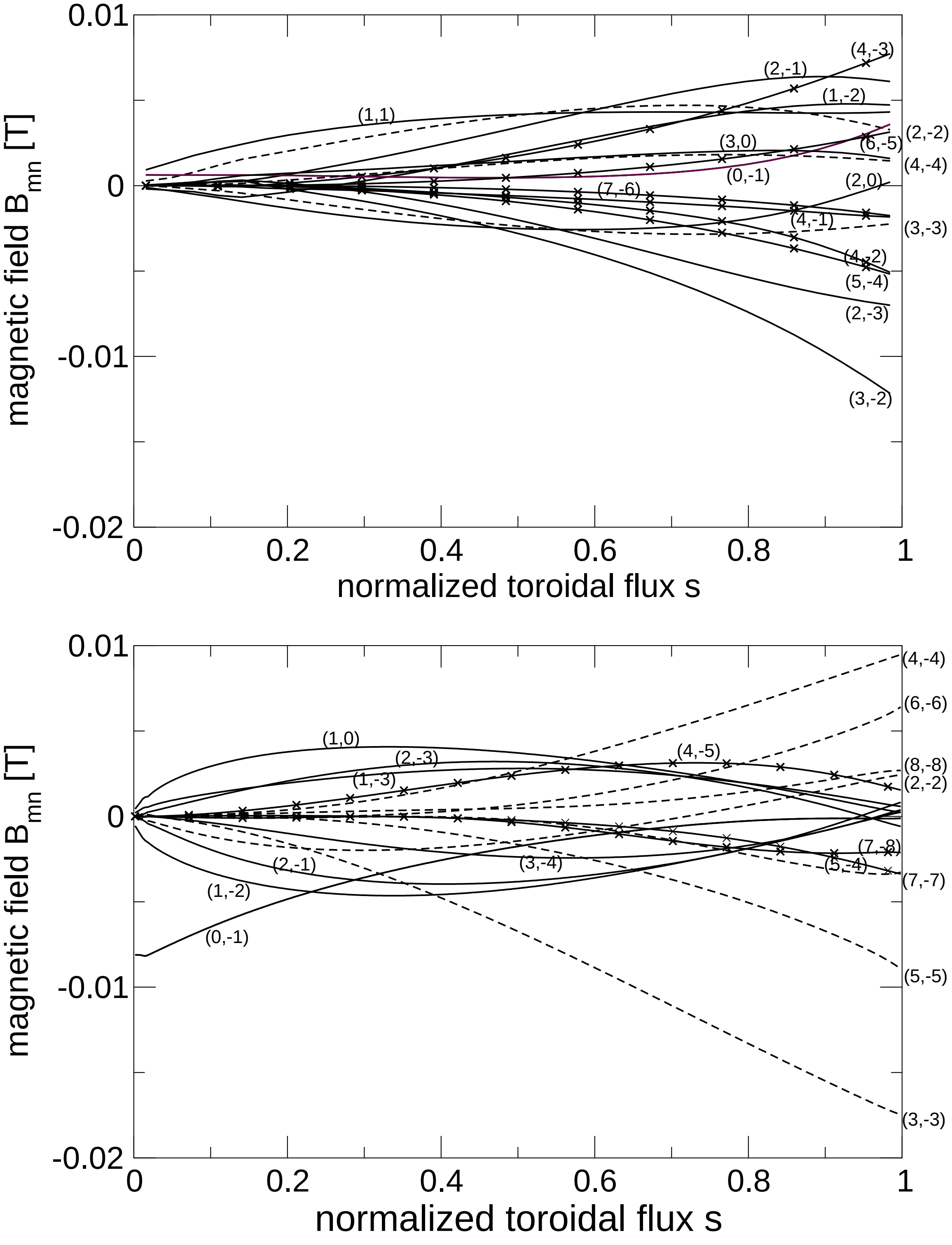
0.01
0
-0.01
-0.02
0
0.2
0.4
0.6
0.8
1
magnetic field $B_{mn}$ [T]
normalized toroidal flux s
(1,1)
(4,-3)
(2,-1)
(1,-2)
(2,-2)
(3,0)
(6,-5)
(4,-4)
(0,-1)
(2,0)
(7,-6)
(4,-1)
(3,-3)
(4,-2)
(5,-4)
(2,-3)
(3,-2)
0.01
0
-0.01
-0.02
0
0.2
0.4
0.6
0.8
1
magnetic field $B_{mn}$ [T]
normalized toroidal flux s
(4,-4)
(6,-6)
(1,0)
(2,-3)
(4,-5)
(8,-8)
(2,-2)
(1,-3)
(7,-8)
(2,-1)
(3,-4)
(5,-4)
(7,-7)
(1,-2)
(0,-1)
(5,-5)
(3,-3)

**Figure 1**

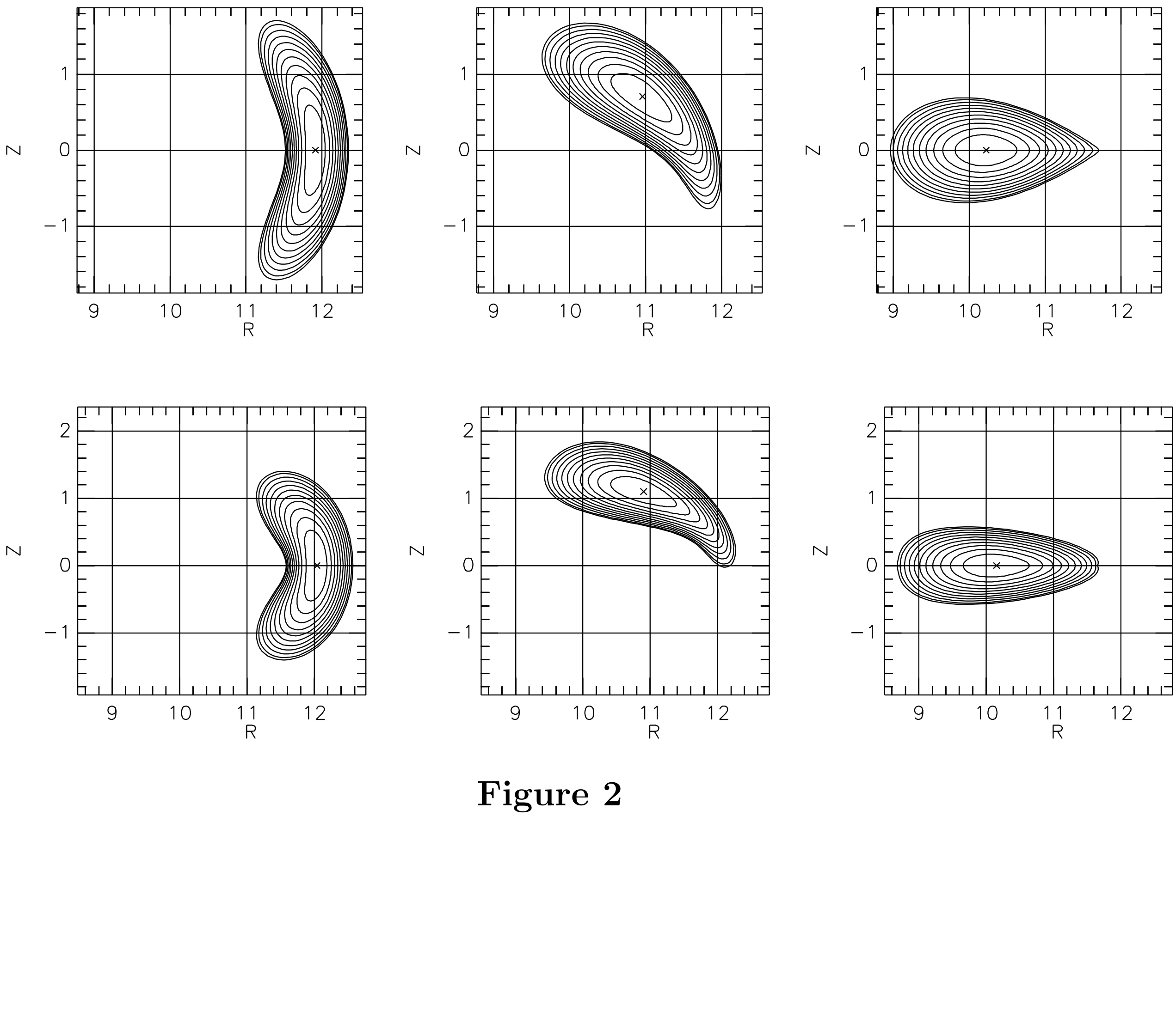


**Figure 2**

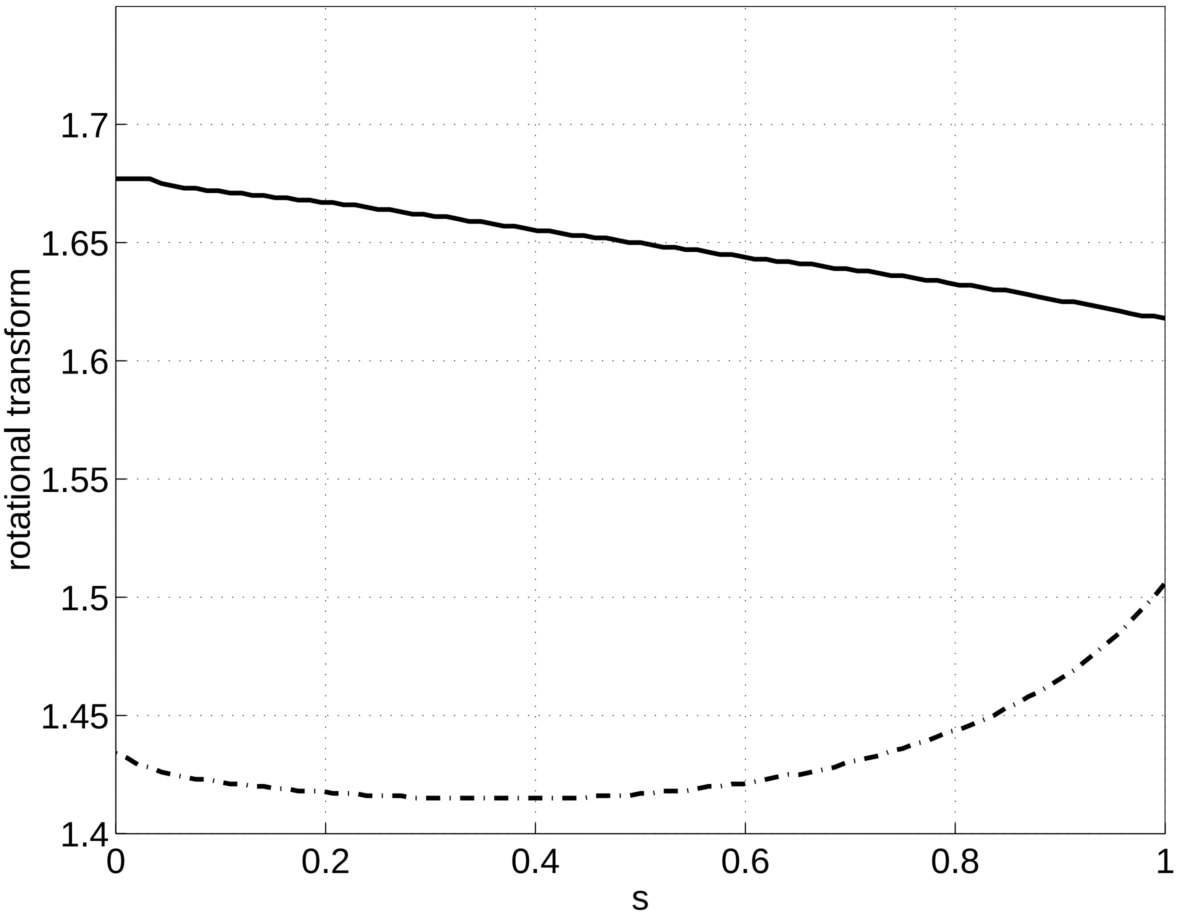


**Figure 3**

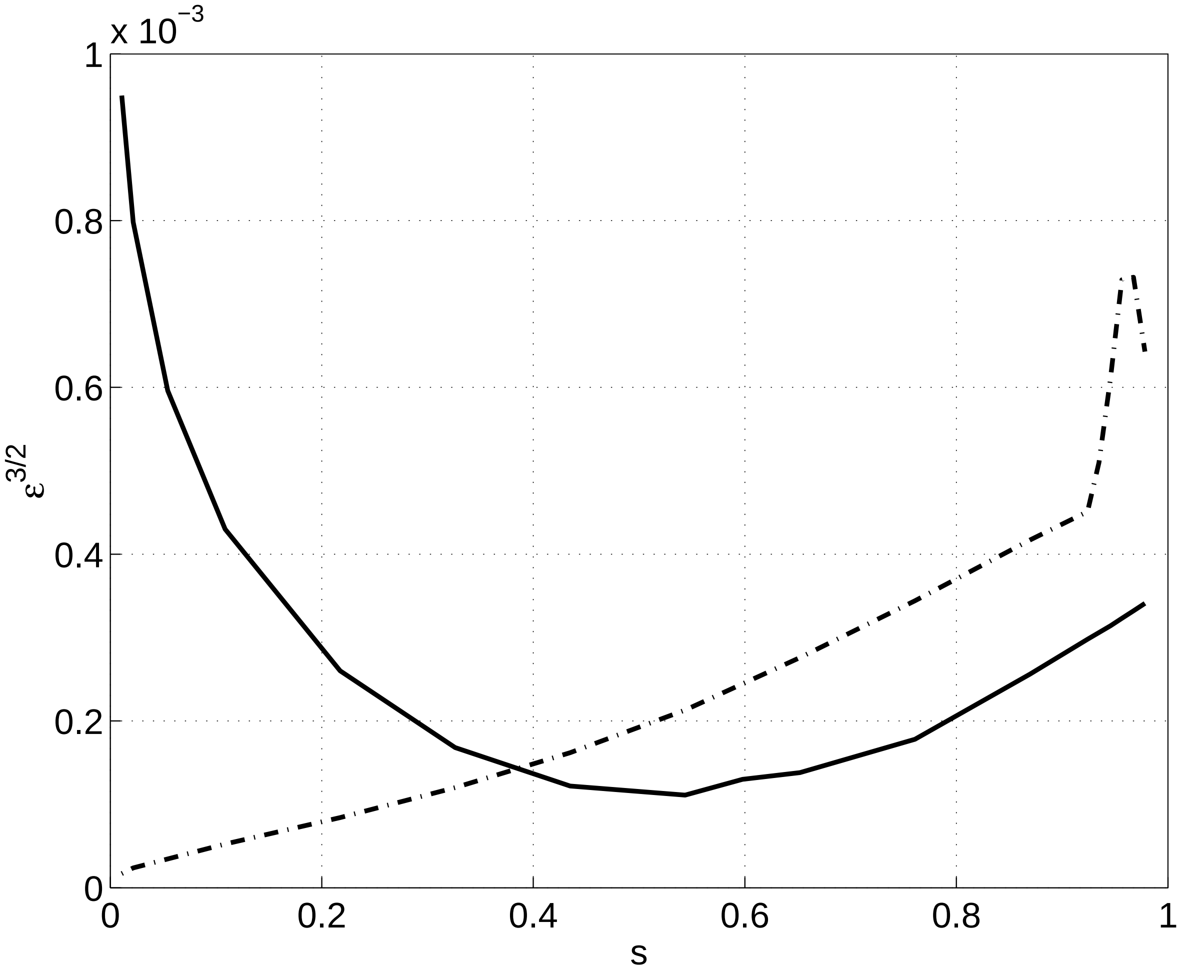


**Figure 4**

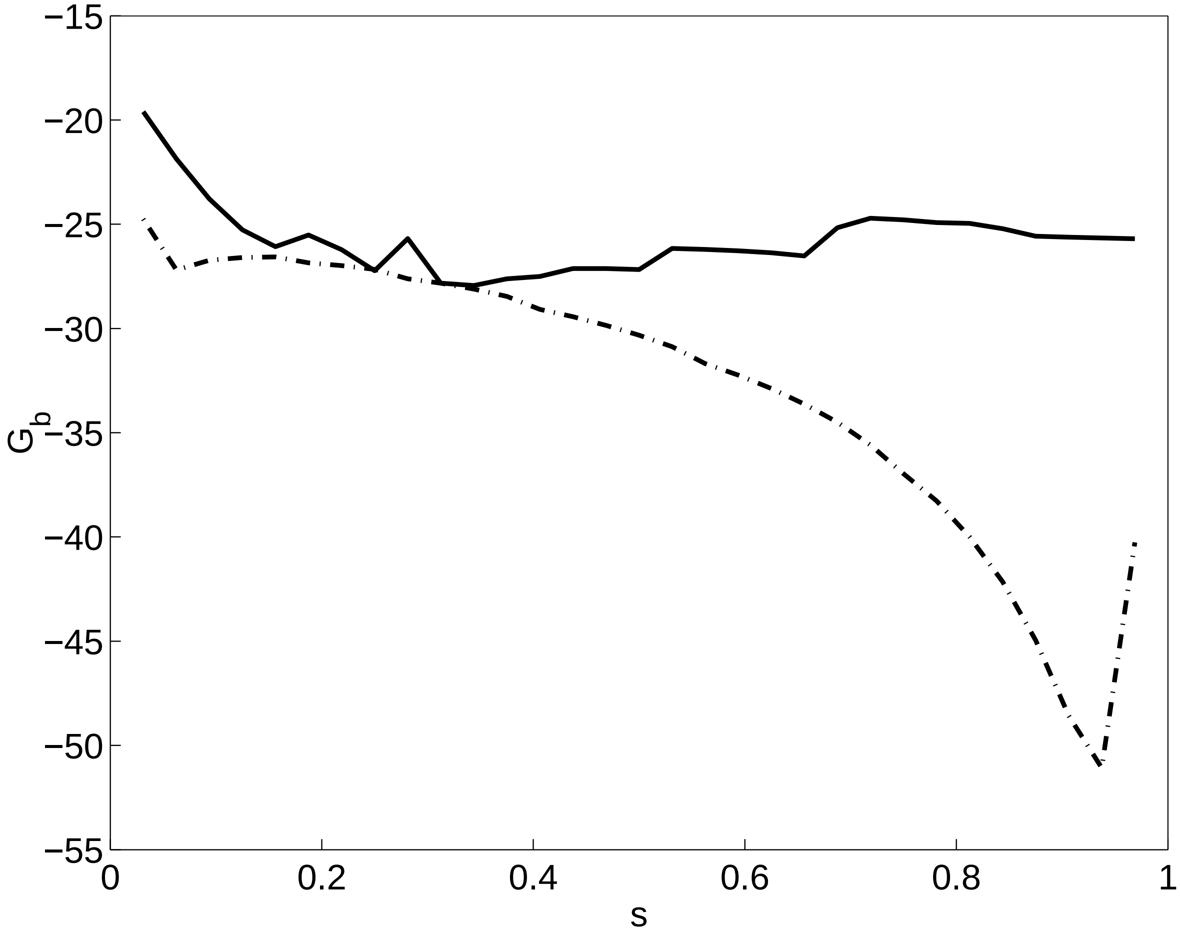


**Figure 5**

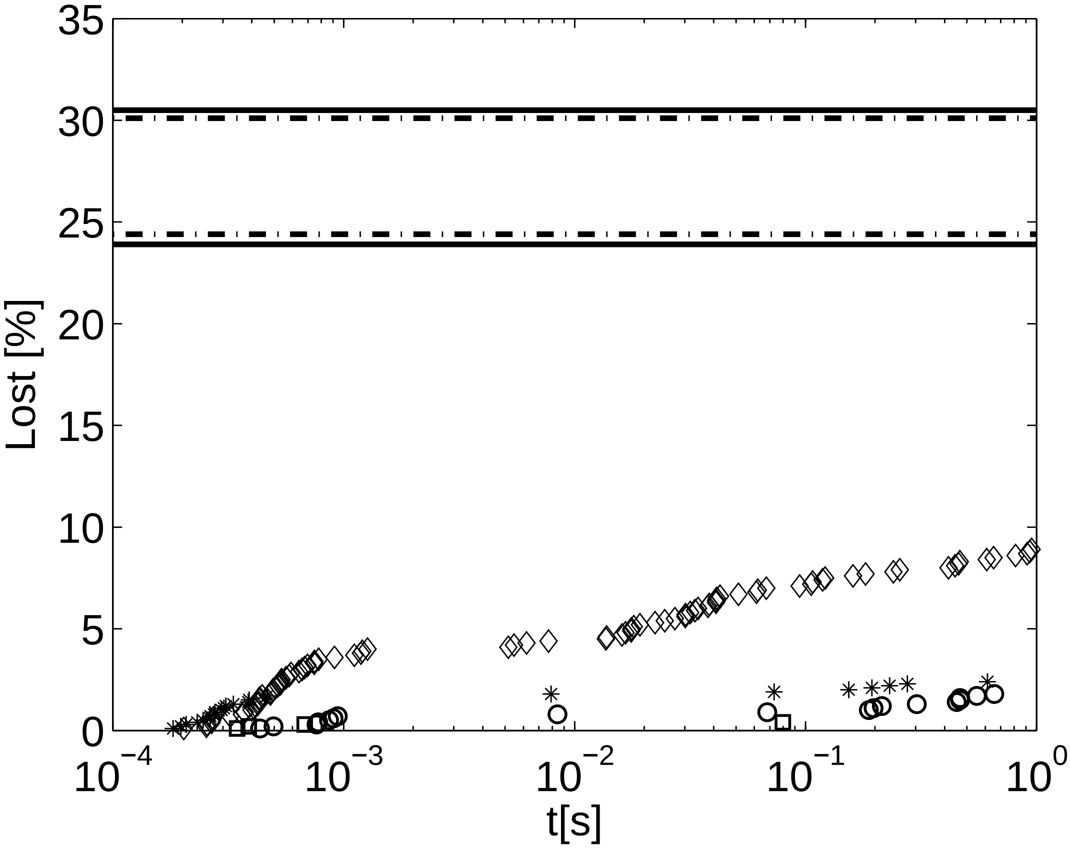


**Figure 6**